IEEE Photonics Journal
An IEEE Photonics Society Publication

Open Access

Generation of the First-Order OAM Modes in Ring Fibers by Exerting Pressure Technology

Volume 9, Number 2, April 2017

Yu Zhang
Fufei Pang
Huanhuan Liu
Xiangqing Jin
Sujuan Huang
Yingchun Li
Jianxiang Wen, *Member, IEEE*
Zhenyi Chen
Min Wang
Tingyun Wang

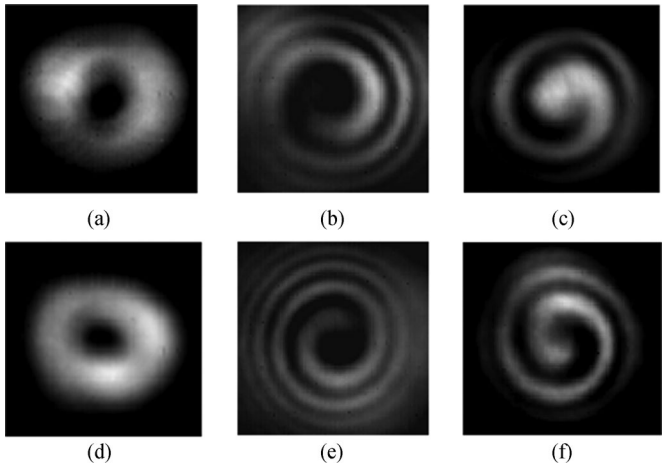

DOI: 10.1109/JPHOT.2017.2677502
1943-0655 © 2017 IEEE

IEEE photonics SOCIETY

IEEE

Generation of the First-Order OAM Modes in Ring Fibers by Exerting Pressure Technology

Yu Zhang, Fufei Pang, Huanhuan Liu, Xiangqing Jin, Sujuan Huang, Yingchun Li, Jianxiang Wen, *Member, IEEE*, Zhenyi Chen, Min Wang, and Tingyun Wang

Key Laboratory of Specialty Fiber Optics and Optical Access Networks, Shanghai University, Shanghai 200072, China

DOI:10.1109/JPHOT.2017.2677502

Manuscript received January 25, 2017; revised February 22, 2017; accepted February 27, 2017. Date of publication March 3, 2017; date of current version March 22, 2017. This work was supported in part by the Natural Science Foundation of China under Grant 61635006, Grant 61422507, and Grant 61605108 and in part by the "Shuguang Program" sponsored by the Shanghai Education Development Foundation and the Shanghai Municipal Education Commission (16SG35). Corresponding author: F. Pang (e-mail: ffpang@shu.edu.cn).

Abstract: We have proposed an effective method of generating the first-order orbital angular momentum (OAM) modes in ring fibers. The first-order OAM modes ($L = \pm 1$) can be represented as the linear superposition of the HE_{21}^{even} mode and the HE_{21}^{odd} mode. Through exerting pressure on the ring fiber by a leverage device, the fundamental mode HE_{11} can be coupled into higher order mode HE_{21} in broadband wavelength ranging from 1530 to 1600 nm. By adjusting the fiber polarization controller and the pressure value exerted on the fiber, both the positive ($L = +1$) and negative ($L = -1$) OAM modes can be generated separately. Moreover, we have demonstrated that the coupling efficiency from the fundamental mode to the first-order OAM modes at wavelength of 1550 nm can reach 67%.

Index Terms: Orbital angular momentum, ring fiber.

1. Introduction

An optical vortex beam having a helical phase wavefront of $e^{iL\theta}$ carries orbital angular momentum (OAM) of $L \cdot \bar{h}$ per photon, where L is topological charge [1], [2]. Due to its unique properties, vortex beams have attracted much attention and shown great potential in a broad range of applications including optical communication [3], [4], optical fiber laser [5], [6], optical micromanipulation [7], [8], quantum science [9], [10], and so on. As for the various applications mentioned above, the main challenge is to generate a good vortex beam. So far, a number of techniques to generate optical vortex beams are mainly based on the using of additional phase elements including spiral phase plates and spatial light modulators [11]. However, these techniques suffer some disadvantages such as severe loss and complexity. On the contrary, generating optical vortex beams in fiber is compatible to the optical communication link since it is easier to be coupled to another fiber than a vortex beam initially created in a free space. Moreover, beams generated in optical fibers are more robust in manipulation and transmission. For example, optical tweezers realized by using optical fibers possess a number of advantages including flexibility and ease in object manipulation

[12], [13]. Also, it is more powerful and less lossy to generate optical vortex beams in fiber to make an optical vortex fiber laser [14]. Therefore, it is preferred to generate optical vortices in fiber directly.

The generation of OAM modes in single-mode fibers (SMFs) can be achieved by introducing pressure on the fiber [15]. However, due to the low coupling efficiency of the input beam into the fiber, the overall coupling efficiency for OAM generation is limited to be ~10%. Recently, many methods for generating OAM modes in specialty fibers have been proposed, such as using long period twisted elliptical fibers [16], making a small core in multimode liquid core optical fiber [17], generating OAM states using fiber Bragg gratings [18], preserving OAM helical Bloch modes in twisted photonic crystal fiber [19], employing two-mode fiber that is initially stressed by a mechanical long-period grating (LPG) for exciting higher-order modes and then stressed by a metal flat slab for OAM modes generation [20], using two-mode fiber to generate optical vortex based on acoustically-induced tunable grating [21]. Compared with the above special fibers, the ring fiber with an annular refractive index (RI) profile is more attractive to generate and transmit OAM modes [22], [23], such as the demonstration of writing micro-bending grating on "vortex fiber" [24]. The reason is that the refractive index profile of a ring fiber could match the intensity profile of vortex beams. Moreover, the ring fiber can generate OAM modes in a broad wavelength range, which is different from the mechanical grating-stressed fibers as well as the acoustically-induced tunable grating fibers that the OAM mode generation is wavelength dependent on the grating period [20], [21], [24]. The existing methods of generating OAM modes in ring fibers are mainly achieved by offset splicing technology [25]. However, the offsetting fibers leak a portion of power of light, which results in a relatively low coupling efficiency of OAM modes. Also, an offset splicing point is fragile that losses the robustness of whole devices. Compared with the offset technology, the pressure technology is more expected because of the advantages to achieve the OAM converter with highly integrated design, high coupling efficiency and robustness.

In this paper, we propose and demonstrate a simple method of generating the first-order OAM modes by exerting pressure on a piece of ring fiber. By applying appropriate pressure value, the higher order mode excitation and the OAM modes generation in the ring fiber can be achieved simultaneously. We show that the OAM modes can be generated in the ring fiber with a high coupling efficiency as well as a broad operation wavelength ranging from 1530 nm to 1600 nm. Importantly, we have demonstrated that the coupling efficiency from the fundamental mode to the first-order OAM modes at wavelength of 1550 nm can reach 67% which is higher than current reports [25]**.** Compared with fibers including single-mode fiber and few-modes fiber by exerting pressure technology for OAM modes generation, our proposed ring fiber with exerting pressure technology is high coupling efficient and highly integrated, which has potential application in object manipulation and optical vortex fiber lasers.

2. Principle

The refractive index profile of the ring fiber is schematically depicted in Fig. 1(a), in which $a_1 = 4\ \mu$m, $a_2 = 7\ \mu$m, $a_3 = 62.5\ \mu$m, $n_1 = 1.465$, $n_2 = 1.47$, and $n_3 = 1.463$. Fig. 1(b) shows the optical microscopic image of the end facet of the ring fiber, which intuitively displays the structure of the ring fiber.

Considering the electric filed distributions of HE_{21}, TM_{01} and TE_{01} modes, the first-order $OAM_{\pm 1,\,1}$ modes be achieved by $\pm\pi/2$-phase shifted linear superposition of the vector mode HE_{21}, and it can also be composed of linear superposition of the vector mode $TM_{01}$and TE_{01} [26]:

$$OAM_{(\pm 1,1)} = \begin{Bmatrix} HE_{21}^{even} + iHE_{21}^{odd} \\ HE_{21}^{even} - iHE_{21}^{odd} \\ TM_{01} + iTE_{01} \\ TM_{01} - iTE_{01} \end{Bmatrix} = F_{(1,1)} \begin{Bmatrix} \hat{\sigma}^{+} e^{+i\theta} \\ \hat{\sigma}^{-} e^{-i\theta} \\ \hat{\sigma}^{-} e^{+i\theta} \\ \hat{\sigma}^{+} e^{-i\theta} \end{Bmatrix} \quad (1)$$

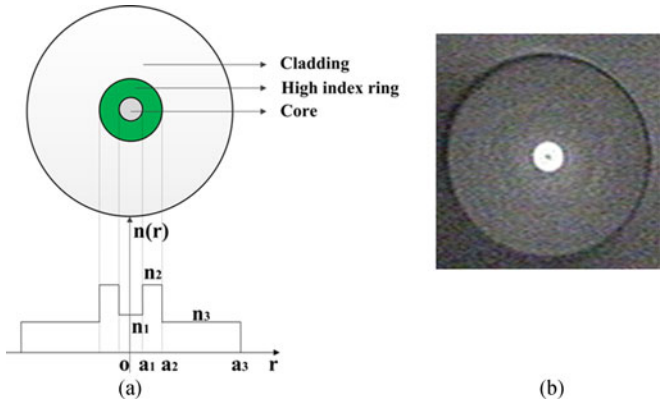

Fig. 1. (a) Schematic diagram of the structure and the refractive index profile of a ring fiber. (b) Microscopic image of the end-facet of the ring fiber.

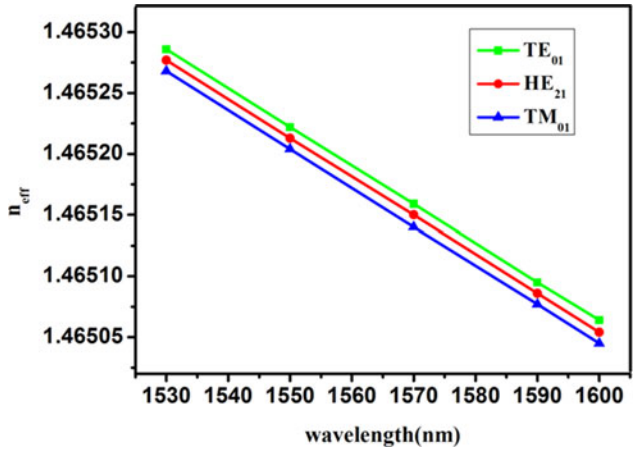

Fig. 2. Effective refractive indices of HE_{21}, TM_{01}, and TE_{01} modes in the ring fiber versus wavelength.

where $\hat{\sigma}^{\pm} = x \pm iy$ represents the left- or right-handed circular polarization of the fiber modes, and $F_{(1,1)}$ refers to the radial wave function for the scalar mode LP_{11}. Note that $TM_{01}$and TE_{01} modes are two eigenmodes with different propagation constants in fibers [4]. Due to the mismatched propagation constants, $TM_{01}$and TE_{01} modes walk off when propagate along the fiber, resulting in unstable OAM modes [26], [27]. In contrast, the first-order $OAM_{\pm 1,1}$ modes can be represented as $\pm\pi/2$-phase shifted linear superposition of the vector modes HE_{21} which have same propagation constant, and thus, there is no walk-off after propagation [22].

The ring fiber with refractive index profile shown in Fig. 1(a) is designed to support 4 modes that are HE_{11}, HE_{21}, TM_{01}, and TE_{01} modes for the first-order OAM modes generation. Fig. 2 compares the calculated effective refractive indices (n_{eff}) of HE_{21}, TM_{01} and TE_{01} modes in the designed ring fiber for OAM modes generation as a function of wavelength. The effective index difference between TE_{01} and HE_{21} mode is 8.96×10^{-6} at the telecommunication wavelength of 1550 nm, while it is 9.49×10^{-6} between TM_{01} and HE_{21} modes.

In this work, we propose to generate $OAM_{\pm 1,1}$ modes by exerting pressure on the ring fiber. Based on (1), $OAM_{+1,1}$ mode could be composed of the left-handed circularly polarized HE_{21} mode, while $OAM_{-1,1}$ could consist of the right-handed circular polarized HE_{21} mode. The basic mechanism of generating OAM modes in the ring fiber by exerting pressure is to excite efficiently the HE_{21} mode and govern the phase difference between the orthogonal modes of HE_{21}^{even} and HE_{21}^{odd} modes.

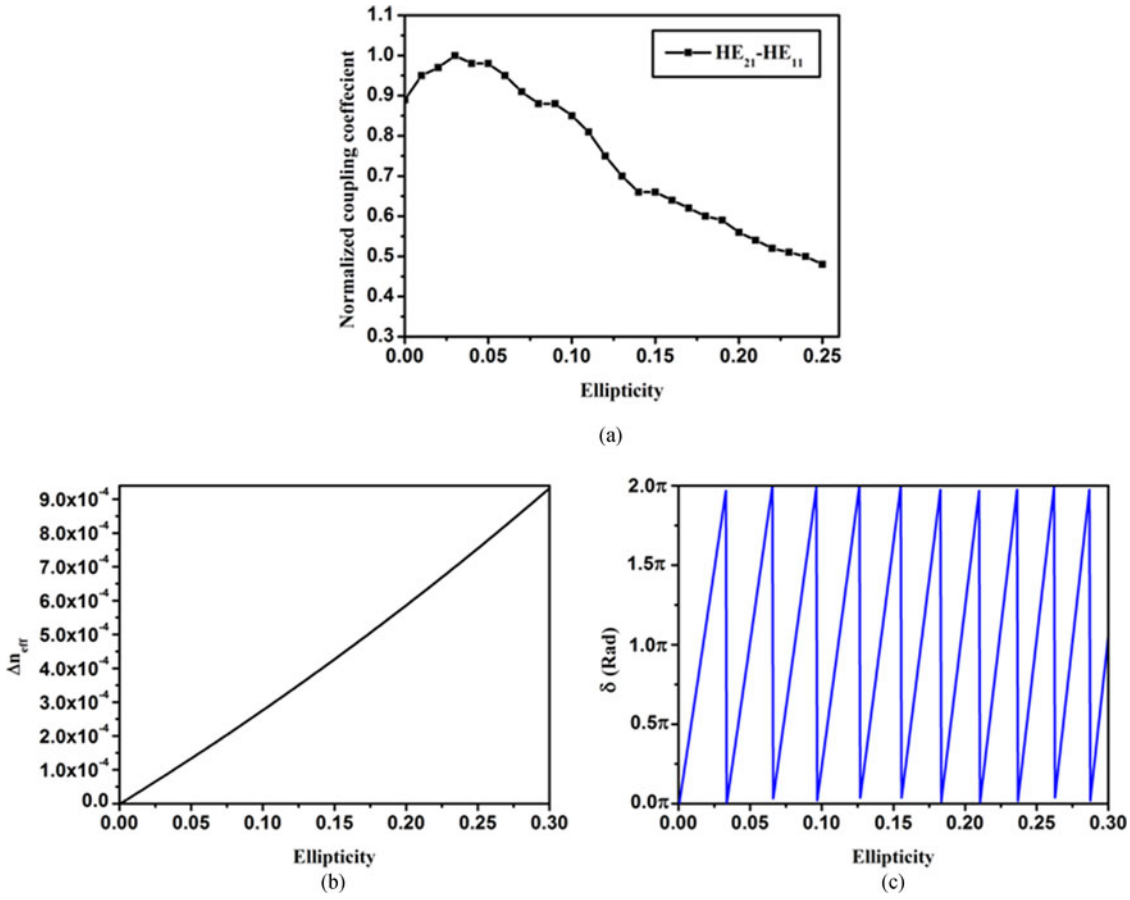

Fig. 3. (a) Normalized coupling coefficient between the fundamental mode HE_{11} and the higher order mode HE_{21} as a function of fiber ellipticity. (b) Δn_{eff}, and (c) δ (phase difference) between HE_{21}^{even} and HE_{21}^{odd} versus the ellipticity of the ring fiber with length of 3.5 cm.

On one hand, the stress by exerting pressure could change the effective dimensions of the ring fiber, thus modifying the propagating constant of the supporting modes. An input HE_{11} mode in the core can be coupled to HE_{21} mode in the ring when the propagation constants of the two modes are comparable and electrical field of the modes are overlapping. On the other hand, the stress on the ring fiber also introduces birefringence into the fiber that interacts with the polarization state of the transmitted light. Due to the destruction of the circular symmetry of the fiber, the HE_{21} mode can be governed to be circularly polarized. Moreover, by adjusting the pressure appropriately, the orthogonal modes of HE_{21}^{even} and HE_{21}^{odd} modes with different phase velocity can achieve a $\pm\pi/2$-phase shift at the end of ring fiber. So that an OAM beam with circularly symmetric annular intensity profile with a helical phase front can be achieved.

By using Comsol software, we study the mode coupling from HE_{11} mode to HE_{21} mode in the ring fiber caused by the pressure. Fig. 3(a) shows the coupling coefficient between the two modes where an elliptical fiber core model is explored. Such coupling coefficient is calculated by the integration of overlapping of electrical fields between the HE_{11} and HE_{21} modes based on well-known coupled-mode theory [28], [29]. It shows that the normalized coupling coefficient varies with the ellipticity, and can be maximized at the fiber ellipticity of $\sim$0.03. Here, the ellipticity is represented by the ratio of the length difference between the semimajor and semiminor axis to the length along the semimajor axis.

Since the pressure also introduces the fiber birefringence, we investigate the influence of fiber ellipticity on the effective refractive index difference (Δn_{eff}) between HE_{21}^{even} and HE_{21}^{odd} modes and

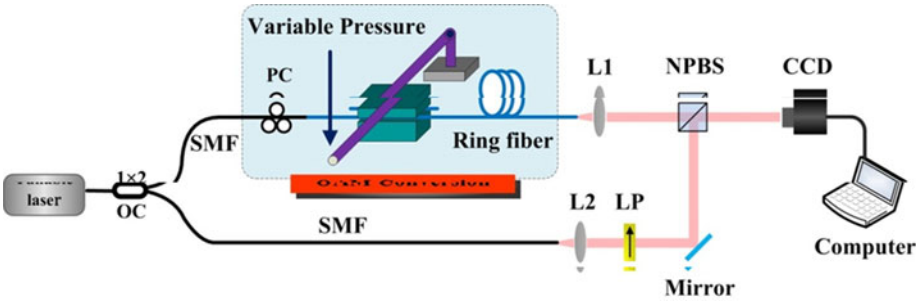

Fig. 4. Experimental setup of generating OAM modes in the ring fiber by exerting pressure on the ring fiber. PC: polarization controller, SMF: single-mode fiber, L(1,2): lens, NPBS: nonpolarizing beam-splitter, CCD: charge-coupled device, LP: linear polarizer.

their phase difference (δ). Fig. 3(b) shows that Δn_{eff} increases with the ellipticity, indicating that HE_{21}^{even} and HE_{21}^{odd} modes are separated by fiber deformation. The relationship between Δn_{eff} and phase difference δ is given as follows:

$$\beta_x - \beta_y = \Delta n_{\text{eff}}.k_0 \tag{2}$$

$$\delta = (\beta_x - \beta_y).z \tag{3}$$

where β_x and β_y are the propagation constants of HE_{21}^{even} and HE_{21}^{odd} modes, respectively; k_0 is the wavenumber in free space; and z is transmission distance of the two modes. Fig. 3(c) shows the theoretical simulation results about phase difference δ which has taken modulus on 2π in relation to the ellipticity of the ring fiber**.** It is found that the change of δ is periodic with the pressure and especially, the period is reduced as the ellipticity increases. Such reduction of period is due to the nonlinear increasing of Δn_{eff} between HE_{21}^{even} and HE_{21}^{odd} modes as fiber ellipticity increases shown in Fig. 3(b)**.** Subsequently, the generation of OAM modes is much easier because multiple values of pressure corresponding to the same phase difference. When the phase difference is 0.5π or 1.5π, a circularly polarized fiber mode HE_{21} carrying the first-order orbital angular momentum can be obtained. Note that the overall coupling efficiency of OAM modes generation is principally limited by the normalized coupling coefficient shown in Fig. 3(a), the phase difference shown in Fig. 3(c) and the length of the deformed ring fiber according to (3). For the deformed ring fiber with length of 3.5 cm determined by the length of flat irons, the simulation results suggest that the optimized values of fiber ellipticity are ~0.033 and ~0.042 for $OAM_{+1,1}$ and $OAM_{-1,1}$ mode generation, respectively.

3. Experimental Setup and Results

Fig. 4 shows the experimental setup of generating the first-order OAM modes in the ring fiber. A 2-m-long ring fiber, a narrow-linewidth (100 kHz) CW tunable laser (Keysight 81600B) with operation wavelength from 1530 nm to 1600 nm, a 50:50 fiber coupler and a fiber polarization controller (PC) are used in this experimental system. The fiber polarization controller is used in the setup system to set the polarization state of the input fundamental mode HE_{11} into linearly polarized. In order to effectively couple the linearly polarized HE_{11} mode into circular polarized HE_{21} mode which corresponds to $OAM_{+1,1}$ or $OAM_{-1,1}$, we propose a simple and efficient way that is exerting pressure on the ring fiber. The ring fiber is placed between two flat irons, and a heavy weight is hung on the leverage to exert pressure on fiber through the leverage device. The length of ring fiber under pressure is about ~3.5 cm and the fiber after exerting pressure is about 1.5 m. To confirm the generation of OAM modes in ring fiber, we use a 50:50 fiber coupler to split a reference beam to observe the phase of the output beam by interfering the output beam with the reference beam. A combination of non-polarizing beam-splitter (NPBS) and a mirror is used to combine the output

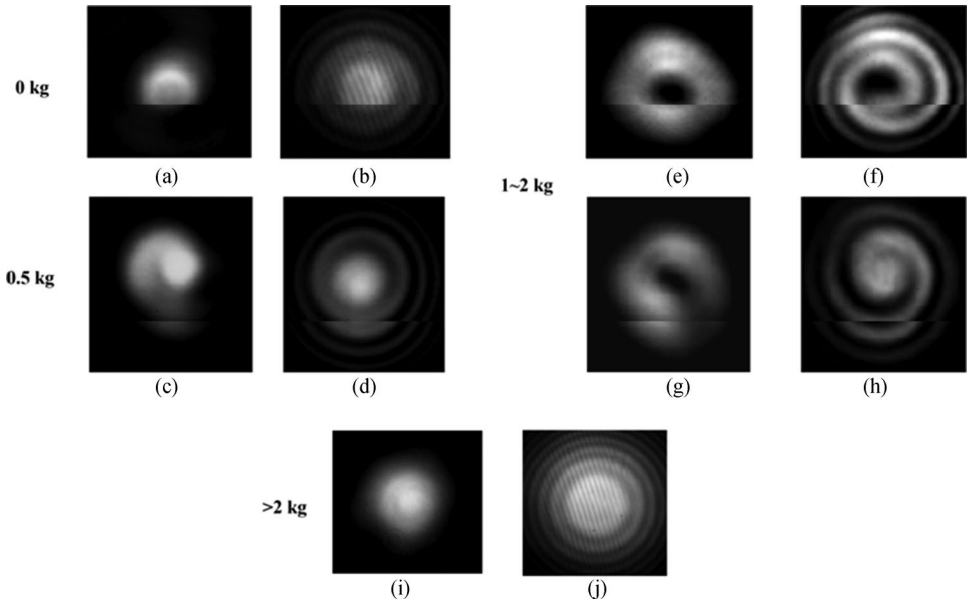

Fig. 5. Intensity and interference pattern of output beams while the heavy weight hung on the lever is (a)–(b) 0 kg, (c)–(d) 0.5 kg, (e)–(h) 1–2 kg, and (i)–(j) >2 kg when the wavelength of input light is 1600 nm.

beam and reference beam. The intensity profile of the output beam and its interference patterns with reference beam are captured by a CCD camera (HAMAMATSU C10633).

In order to generate good OAM modes, we need to suppress HE_{11} mode by coupling it into HE_{21} mode. In addition, in order to make sure the pressure is exerted well and truly on the fiber's central axis, we put another short parallel ring fiber between two flat irons and then tuning the direction of the force to make sure the force acting on the fiber is uniform otherwise the applied force is easy to deviate from the central axis. Because fiber circular symmetry is broken by the pressure applied rightly on the central axis, the fundamental mode HE_{11} can be coupled into higher-order mode HE_{21}. By controlling the pressure forced on the ring fiber, the polarization will be changed. When the phase difference is 0.5π *or* 1.5π, the linear polarization state will become circular polarization state and the first-order OAM modes will be generated.

As the fiber ellipticity has an important influence on the generation of OAM modes, several heavy weights are used to exert different magnitude of pressure during the experiment. Fig. 5 shows the intensity of the output beams from the end of ring fiber as well as the interference patterns with the reference beam. As shown in Fig. 5(a) and (b), when there is no pressure forced on fiber, only HE_{11} exists in the ring fiber, and the observed interference pattern of concentric circles demonstrates that the output beam carries no orbital angular momentum. As shown in Fig. 5(c) and (d), it can be found that when the weight is small (0-0.5 Kg), the intensity of the output beam changes slightly. The interference pattern of concentric circles indicates that there is weak orbital angular momentum generated. However, when the weight is middle (1-2 kg), the good OAM modes ($L = \pm 1$) fields with donut-like shape are observed, as shown in Fig. 5(e) and (g). The interference pattern varies slightly with time, demonstrating a good stability of OAM modes in the 1.5-m-long ring fiber after the pressure region. Moreover, the typical spiral interference patterns are observed as shown in Fig. 5(f) and (h), which confirms the generation of OAM modes in the ring fiber. By further increasing the weight, the intensity of the output beam will change back to the pattern of HE_{11} mode due to the over coupling as shown in Fig. 5(i) and (j). Therefore, the good OAM modes can be obtained when the heavy weight ranges from 1 kg to 2 kg.

The overall coupling efficiency from the fundamental mode HE_{11} to the first-order OAM modes is estimated by calculating the ratio of the output light power at the end of the ring fiber to the

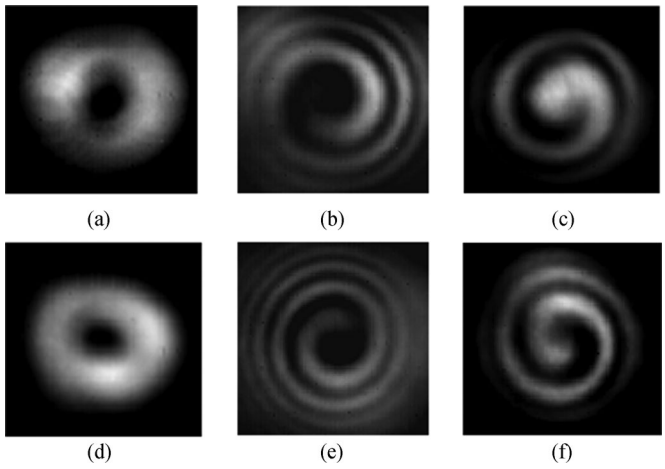

Fig. 6. (a) Intensity of the first-order OAM modes and interference patterns of OAM modes with (b) L = +1 and (c) L = –1 when the wavelength of input light is 1530 nm. (d) Intensity of the first-order OAM modes and interference patterns of OAM modes with (e) L = +1 and (f) L = –1 when the wavelength of input light is 1550 nm.

light power at the input of the ring fiber. The coupling efficiency is calculated to be 67% under the optimized value of pressure exerting on the ring fiber. Such 67% coupling efficiency is higher than the exciting of LP_{11} in a liquid core optical fiber (35%) [17] and the first-order OAM modes in the ring fiber (7.5%) [25]. We have also investigated the influence of fiber length on the coupling efficiency. Three kinds of flat irons are taken whose lengths are 1 cm, 3.5 cm and 5 cm, respectively. The optimized coupling efficiencies for the three cases are all achieved to be ~67% by individually applying appropriate pressure value as well as carefully adjusting the polarization state. It indicates that the fiber ellipticity is the key parameter for excellent OAM generation rather than the length of the deformed ring fiber in such a short and straight format. Therefore, in order to further increase the coupling efficiency, the pressure value is key parameter that should be precisely controlled. Moreover, the loss originated from the splicing point between the single mode fiber and ring fiber is ~0.22 dB which needs to be minimized through the good alignment between the SMF and ring fiber as well as the careful control of the intensity and the duration of arc discharge.

The purity of the OAM modes is further investigated by including the polarization beam displacing prism to project different polarization, and the value is calculated based on the "ring" technique [24], [30]. In the "ring" technique, azimuthal intensity profile of left and right circular projection for a certain radius are measured and then taking the Fourier series of the intensity profile, afterwards the Fourier series coefficients can be used to calculate the purity of OAM modes. The fundamental frequency component contains the information of interferences between HE_{21} and HE_{11} modes, while the second-order frequency component refers to the interferences between HE_{21} and combined modes of TM_{01} and TE_{01} modes. The purity is calculated to be 61% for the HE_{21} mode and 27% for the combined modes of TM_{01} and TE_{01}. Also, the purity of the HE_{11} mode is 4%. The observation that the HE_{21} mode mainly contributes to the OAM modes generation in the proposed ring fiber is based solely upon the condition that the ring fiber has high refractive index contrast between the ring and cladding while the exerting pressure is well controlled. Additionally, when the structure of the ring fiber changes, the technology is still applicable provided the high-contrast refractive index of the ring fiber is ensured and the exerted pressure is appropriate.

By the same technique, the OAM modes actually can be generated from 1530 nm to 1600 nm in the same ring fiber under the same pressure value. When the wavelength is set to be 1530 nm, the intensity of the first-order OAM modes is shown in Fig. 6(a) and interference patterns of OAM modes with L = +1 and L = − 1 are shown in Fig. 6(b)-(c). Similarly, the intensity and interference patterns of the first-order OAM modes at 1550 nm are shown in Fig. 6(d)-(f). The coupling efficiencies at

1530 nm and 1550 nm are close to the one achieved at 1600 nm. Due to the fiber splicing as well as the leakage of pressure-induced leaky higher-order modes, light propagating along the ring fiber experiences an excess loss of ~1.74 dB. The results confirm that the ring fiber can generate OAM modes in a broad wavelength range, which is different from the mechanical grating-stressed fibers that the operation wavelength is limited by the grating period [20], [24]. It is believed that the proposed method for generating broadband first-order OAM modes in ring fiber by exerting pressure can be also extended to higher-order OAM modes. In this case, the fiber structure should be well designed to support higher-order mode and the fiber ellipticity should be well controlled.

4. Conclusion

We have demonstrated the ring fiber for the generation and transmission of OAM modes. Such ring fiber is superior to SMF or few-modes fiber when using pressure technology because of the annular refractive index profile. Besides, by applying the appropriate pressure on the ring fiber, the fundament mode HE_{11} is successfully coupled into the first-order OAM modes whose purity can be increased by adjusting the fiber polarization controller as well as the pressure value exerted on the ring fiber. The results demonstrate that the good OAM modes ($L = \pm 1$) can be obtained in a broad wavelength ranging from 1530 nm to 1600 nm, and the coupling efficiency of the first-order OAM modes can be up to 67%, which shows an effective method to generate OAM modes. The proposed simple, broad wavelength and versatile OAM converter may see potential applications in particles trapping, optical vortex laser and *etc*. Furthermore, in order to further extend the applications of OAM modes in which the relatively long length of ring fiber is needed, the structure of ring fiber could be redesigned with an improved refractive index contrast.

References

[1] L. Allen, M. W. Beijersbergen, R. J. C. Spreeuw, and J. P. Woerdman, "Orbital angular momentum of light and the transformation of Laguerre-Gaussian laser modes," *Phys. Rev. A.*, vol. 45, no. 11, pp. 8185–8189, Jun. 1992.

[2] A. M. Yao and M. J. Padgett, "Orbital angular momentum: Origins, behavior and applications," *Adv. Opt. Photon.*, vol. 3, no. 2, pp. 161–204, May 2011.

[3] D. Ma and X. Liu, "On the orbital angular momentum based modulation/demodulation scheme for free space optical communications," in *Proc. Int. Conf. Wireless Commun. Signal Process.*, Oct. 2015, pp. 1–6.

[4] N. Bozinovic *et al.*, "Terabit-scale orbital angular momentum mode division multiplexing in fibers," *Science*, vol. 340, no. 6140, pp. 1545–1548, Jun. 2013.

[5] Z. Lin *et al.*, "Generation of optical vortices using a helical fiber Bragg grating," *J. Lightw. Technol.*, vol. 32, no. 11, pp. 2152–2156, Jun. 2014.

[6] J. Hamazaki, R. Morita, K. Chujo, Y. Kobayashi, S. Tanda, and T. Omatsu, "Optical-vortex laser ablation," *Opt. Exp.*, vol. 18, no. 3, pp. 2144–2151, Feb. 2010.

[7] K. Toyoda, K. Miyamoto, N. Aoki, R. Morita, and T. Omatsu, "Using optical vortex to control the chirality of twisted metal nanostructures," *Nano Lett.*, vol. 12, no. 7, pp. 3645–3649, Jun. 2012.

[8] A. Lehmuskero, Y. M. Li, P. Johansson, and M. Käll, "Plasmonic particles set into fast orbital motion by an optical vortex beam," *Opt. Exp.*, vol. 22, no. 4, pp. 4349–4356, Feb. 2014.

[9] E. Nagali *et al.*, "Quantum information transfer from spin to orbital angular momentum of photons," *Phys. Rev. Lett.*, vol. 103, no. 1, pp. 013601-1–013601-4, Jul. 2009.

[10] L. Marrucci *et al.*, "Spin-to-orbital conversion of the angular momentum of light and its classical and quantum applications," *J. Opt.*, vol. 13, no. 6, pp. 064001–064013, Apr. 2011.

[11] A. Kumar, P. Vaity, J. Banerji, and R. P. Singh, "Making an optical vortex and its copies using a single spatial light modulator," *Phys. Lett. A.*, vol. 375, no. 41, pp. 3634–3640, Sep. 2011.

[12] K. S. Abedin, C. Kerbage, A. Fernandez-Nieves, and D. A. Weitz, "Optical manipulation and rotation of liquid crystal drops using high-index fiber-optic tweezers," *Appl. Phys. Lett.*, vol. 91, no. 9, pp. 091119-1–091119-3, Aug. 2007.

[13] Z. Liu, C. Guo, J. Yang, and L. Yuan, "Tapered fiber optical tweezers for microscopic partical trapping: Fabrication and application," *Opt. Exp.*, vol. 14, no. 25, pp. 12510–12516, Dec. 2006.

[14] T. Omatsu, "Optical vortex fiber lasers and their application to material nano-processing," presented at the Lasers & Electro-optics (CLEO) 2013, pp. CTu3K.3-1-CTu3K.3-2.

[15] D. McGloin, N. B. Simpson, and M. J. Padgett, "Transfer of orbital angular momentum from a stressed fiber-optic waveguide to a light beam," *Appl. Opt.*, vol. 37, no. 3, pp. 469–472, Jan. 1998.

[16] C. N. Alexeyev, T. A. Fadeyeva, B. P. Lapin, and M. A. Yavorsky, "Generation and conversion of optical vortices in long-period twisted elliptical fibers," *Appl. Opt.*, vol. 51, no. 10, pp. C193–C197, Mar. 2012.

[17] W. Gao, X. Hu, C. Mu, and P. Sun, "Generation of vector vortex beams with a small core multimode liquid core optical fiber," *Opt. Exp.*, vol. 22, no. 9, pp. 11325–11330, Jul. 2014.

[18] L. Wang, P. Vaity, B. Ung, Y. Messaddeq, L. A. Rusch, and S. LaRochelle, "Characterization of OAM fibers using fiber Bragg gratings," *Opt. Exp.*, vol. 22, no. 13, pp. 15653–15661, Jun. 2014.
[19] X. M. Xi *et al.*, "Orbital-angular-momentum-preserving helical Bloch modes in twisted photonic crystal fiber," *Optica*, vol. 1, no. 3, pp. 165–169, Aug. 2014.
[20] S. Li, Q. Mo, X. Hu, C. Du, and J. Wang, "Controllable all-fiber orbital angular momentum mode converter," *Opt. Lett.*, vol. 40, no. 18, pp. 4376–4379, Sep. 2014.
[21] W. Zhang *et al.*, "Optical vortex generation with wavelength tunability based on an acoustically-induced fiber grating," *Opt. Exp.*, vol. 24, no. 17, pp. 19278–19285, Aug. 2016.
[22] Y. Yue *et al.*, "Mode properties and propagation effects of optical orbital angular momentum (OAM) modes in a ring fiber," *IEEE Photon. J.*, vol. 4, no. 2, pp. 535–543, Apr. 2012.
[23] P. Gregg, P. Kristensen, and S. Ramachandran, "13.4 km OAM state propagation by recirculating fiber loop," *Opt. Exp.*, vol. 24, no. 17, pp. 18938–18947, Aug. 2016.
[24] N. Bozinovic, S. Golowich, P. Kristensen, and S. Ramachandran, "Control of orbital angular momentum of light with optical fibers," *Opt. Lett.*, vol. 37, no. 13, pp. 2451–2453, Jul. 2012.
[25] X. Jin, F. Pang, Y. Zhang, and S. Huang, "Generation of the first-order OAM modes in single-ring fibers by offset splicing technology," *IEEE Photon. Technol. Lett.*, vol. 28, no. 14, pp. 1581–1584, Jul. 2016.
[26] H. Xu and L. Yang, "Conversion of orbital angular momentum of light in chiral fiber gratings," *Opt. Lett.*, vol. 38, no. 11, pp. 1978–1980, Jun. 2013.
[27] P. Z. Dashti, F. Alhassen, and H. P. Lee, "Observation of orbital angular momentum transfer between acoustic and optical vortices in optical fiber," *Phys. Rev. Lett.*, vol. 96, no. 4, p. 043604, Feb. 2006.
[28] R. Olshansky, "Mode coupling effects in graded-index optical fibers," *Appl. Opt.*, vol. 14, no. 4, pp. 935–945, Mar. 1975.
[29] T. Erdogan, "Cladding-mode resonances in short- and long-period fiber grating filters," *J. Opt. Soc. Amer. A.*, vol. 14, no. 8, pp. 1760–1773, Aug. 1997.
[30] S. Ramachandran and P. Kristensen, "Optical vortices in fiber," *Nanophotonics*, vol. 2, no. 5–6, pp. 455–474, Dec. 2013.